

Local Temperature Measurements on Full-Size Systems in the Laboratory: Insight into the Extent of Thermal Bridges in Building Envelope Components

*Thomas W. Petrie, Jan Koňny, Jerald A. Atchley and André O. Desjarlais
Buildings Technology Center, Oak Ridge National Laboratory*

ABSTRACT

Techniques that can be applied during hot box measurement of total system thermal performance provide insight into the extent of thermal bridges and the effectiveness of measures taken to eliminate them. The techniques comprise extensive measurements of local temperatures on surfaces near thermal bridges and substitution of simple elements for complicated elements of the test section construction.

Three examples present results of local temperature measurements near thermal bridges in terms of dimensionless ratios $(T - T_{\text{air out}})/(T_{\text{air in}} - T_{\text{air out}})$. Away from the thermal bridges, the ratios approach 1.0 on the inside of the test section and 0.0 on the outside. How far the ratios are from 0.0 or 1.0 is evidence of the strength of the thermal bridges. Conversely, how close they are to the limits shows the effectiveness of measures taken to eliminate the thermal bridges.

Good agreement between local temperature measurements and predictions by three-dimensional models of the construction near the thermal bridges allows models to predict local heat transfer through complicated elements. Rate of heat flow through simple elements can be determined by their known geometry, thermal resistance of their construction materials and measurement of temperature differences across them. By measuring the difference between overall system performance with complicated elements and with simple ones, rate of heat flow through the complicated elements can be determined independently of models.

Introduction

The evolution of thermally efficient building envelopes has progressed to the point where attention must be focused on details. Insulation in the form of blankets, batts, boards and loose-fill materials allows walls to be designed with high levels of thermal resistance. Windows and doors, as well as their frames, are available in configurations offering necessary form and function without sacrificing good thermal performance.

The thermal performance of details (where the walls, roofs and floors are joined and the window and door frames are installed) is dominated by the presence of structural materials needed for strength. Details exhibit thermal bridges unless care is taken in design and construction to reduce the thermal effects of the dense, lower thermal resistance, structural materials. Understanding the thermal performance of these construction details requires measurements and modeling to characterize the nature and extent of the thermal bridging. Additional measurements and modeling are frequently needed to follow up on proposed improvements.

Significant progress has been made in characterizing residential building envelopes. An overall indicator of the thermal performance of a residential building envelope is available at the Internet web site <http://www.ornl.gov/roofs+walls/whole_wall>. The whole-wall calculator at this site provides an on-line, interactive method for determining the whole-wall R-value for a

variety of wall systems and user-defined, custom house plans. The method is described in detail in several technical articles (Kohny & Desjarlais 1994) culminating in a featured article in the ASHRAE Journal (Christian & Kohny 1996). The purpose of the method is to establish a realistic energy savings metric for consumers faced with the decision of what wall system to select for a building they are buying or building. There are many alternatives to dimensional wood-framed wall construction now available, including steel framing, low-density concretes, structural insulated core panels, insulated concrete forms, and even straw bales. Comparisons of energy performance can hardly be accurate unless the effects of all details are included in the energy performance metric.

The whole-wall thermal resistance or R-value is an important part of a metric for the energy performance of the entire building envelope. Thermal resistance, even when expanded to include the effects of all interface details, remains a property of a particular combination of components. The same number will apply in any climate, if appropriate account is taken for the dependence upon temperature of the thermal conductivity of individual materials.

This paper deals with an issue inherent in the Internet calculator and considerations of whole building performance. It concerns measurement techniques used to understand thermal bridges in hot box experiments. Along with two-dimensional and three-dimensional modeling, these techniques provide insight into the extent of thermal bridges and the effectiveness of measures taken to eliminate them. This paper seeks to show, by examples, how measurements and models complement measurements of overall thermal performance by hot box techniques.

Examples will be presented from work related to the whole-wall thermal performance calculator but carried out at the Buildings Technology Center at the Oak Ridge National Laboratory since the calculator appeared on the Internet. One example deals with a type of wood-framed manufactured housing that has a short heel where the roof rafters meet the ceiling joists. There is little room for conventional batt insulation or blown-in insulation at the eave edge. Another example is a C-shaped steel-framed attic built like a wood-framed attic and then retrofitted for some breaking of the thermal bridges through the joists and through the top plate at the eave edge of the attic. A third example deals with a parapet wall made from heavyweight concrete with a foam insulation core. It is thermally resistive to horizontal heat flow but the foam insulation core is ineffective in preventing heat flow vertically at the wall-ceiling interface.

Local Temperature Measurements in Hot Box Tests

A hot box test is the laboratory measurement of heat transfer through a specimen under controlled air temperature, air velocity and thermal radiation conditions. The conditions are established in a metering chamber on one side of the specimen and in a climatic chamber on the other side. Figure 1 shows schematically the Large Scale Climate Simulator (LSCS) for the testing of horizontal test sections (mostly commercial and residential roofs) at the Oak Ridge National Laboratory's Buildings Technology Center. There is enough space in the upper chamber to accommodate sloped roof assemblies, such as the actual half roof of a manufactured home shown in Fig. 1.

Standard methods for hot box tests are addressed by ASTM Designation C 1363 and the older C 236 and C 976 (ASTM 1997, ASTM 1989, ASTM 1990). These standard test methods concern the accurate determination of overall thermal performance of the specimen. Temperature variations across the metered area are recognized as a fact of operation with specimens large enough to represent a full-sized component of a building envelope. The methods caution that

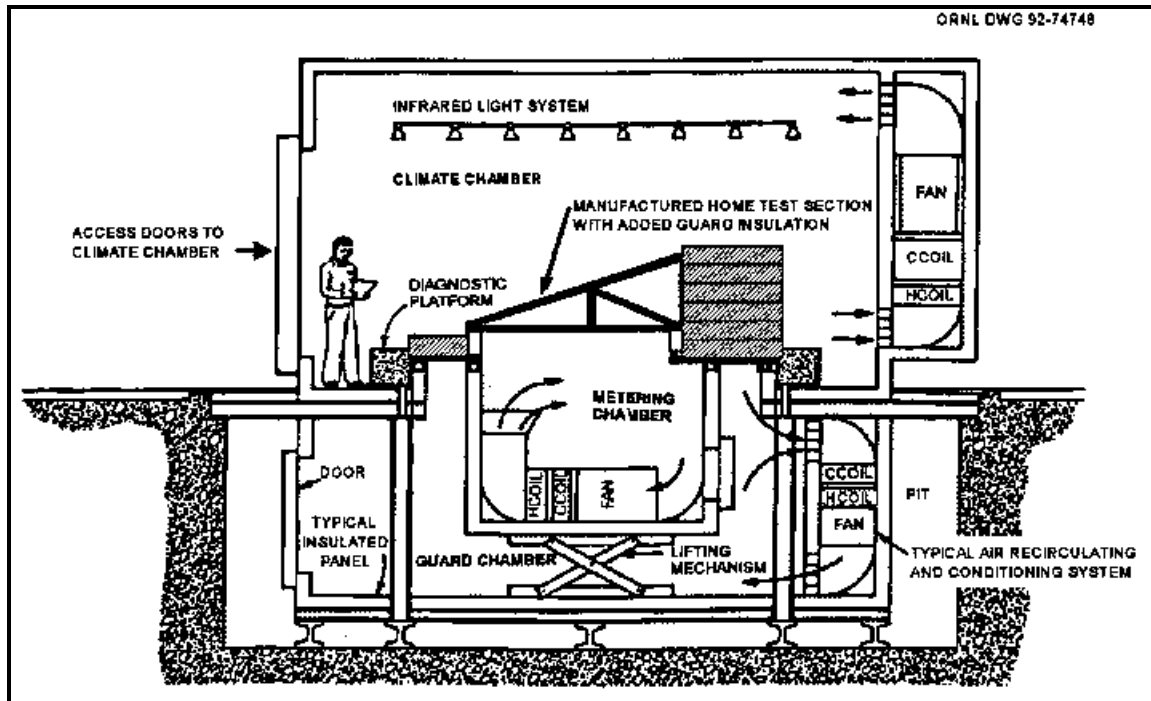


Figure 1. Schematic of the Large Scale Climate Simulator with a Manufactured Home Test Section in Place between the Climatic and Metering Chambers

so that a reliable area weighted mean surface temperature may be obtained.

Another use we have found for additional temperature sensors is to validate three-dimensional models of test specimens. The purpose of the models is to predict the local heat transfer through components or through features of the specimen for which direct measurement of heat transfer is difficult. The smallest heat flux transducer we have found convenient to use is 5.1 cm square and it is accurate only when used in the same situation as that in which it is calibrated: one-dimensional heat flow through the same materials as present in the specimen. The additional temperature sensors provide critical checks on the reasonableness of the model. Even though the model uses the same boundary conditions as were imposed in the tests, such as air temperatures measured inside and outside the test section, agreement between measured and modeled surface temperatures is required over the entire area of the test section. This ensures that the correct temperature differences and heat transfer parameters, such as local heat transfer coefficients, are imposed in the model to drive local heat transfer.

There is a situation where the heat transfer for part of a test section can be measured directly. In complicated test sections, certain features of the test section can be replaced by simple elements like foam insulation with known, homogeneous thermal resistance. The control system for the Large Scale Climate Simulator allows us to duplicate conditions precisely from test to test if desired. Tests at duplicate conditions with a complicated feature and then with a simple feature allow the respective test section heat flow rates to be subtracted for the effect of the complicated feature. Additional temperature sensors ensure that the conditions are indeed duplicated as far as the feature of interest is concerned. They also permit calculation of the heat flow through the simple element from measured temperature differences multiplied by surface area and divided by thermal resistance.

In the examples that follow, local surface temperatures will be presented at various

locations on three different systems studied in the Large Scale Climate Simulator. For convenient comparisons among the examples, which were tested at widely varying conditions, a local temperature, T , is presented in dimensionless form. Dimensionless temperature is defined as the ratio $(T - T_{\text{air out}})/(T_{\text{air in}} - T_{\text{air out}})$. The examples will show that this ratio is not sensitive to the magnitude of the normalizing difference $(T_{\text{air in}} - T_{\text{air out}})$. The local temperatures, T , lie between $T_{\text{air in}}$ and $T_{\text{air out}}$ so the ratio will be between 0 and 1. In the absence of a thermal bridge, even with the severe temperature differences imposed in many of the tests, heat fluxes are low for these systems. The reason is that they are generally well-insulated as measured by the insulation levels in the center of their walls and roofs. The temperature ratios for surfaces exposed to $T_{\text{air out}}$ will generally be less than 0.05 without a thermal bridge. The ratio for surfaces exposed to $T_{\text{air in}}$ will generally be greater than 0.95 without a thermal bridge.

Eave Edge of Manufactured Home Roof

The manufactured home test section is an example of a test section where detailed local temperature measurements helped to validate a model of three-dimensional heat flow through part of the test section. Figure 2 is a schematic of the eave edge of the half-roof test section, shown in place in Fig. 1. The side wall is constructed from nominal 2x4 wood studs, 61 cm on center, with a nominal 2x4 wood top plate. Gypsum board is on the interior and unsheathed aluminum siding on the exterior with fiberglass batt insulation in the cavity. The attic trusses are constructed from nominal 2x2 wood framing, also 61 cm on center, with a nominal 1x3 perimeter rail (6.4 cm high). The ceiling is gypsum board attached to the trusses so that it extends underneath the perimeter rail. At the time this test specimen was made, nominal insulation of the production homes it modeled was two layers of fiberglass batt insulation, each layer 5.7 cm thick when fully expanded with nominal thermal resistance of 1.23 m²·K/W. This thickness is enough that the two layers were compressed at the eave edge of the roof between the gypsum board ceiling and the metal roof when it was put in place over the trusses. The insulation was compressed until a horizontal distance of 10.5 cm from the inside wall.

In our study we were interested in how much of the heat flow for the whole test section flowed through the stub of eave wall (H in Fig. 2) and how much through the area where the insulation was compressed (V in Fig. 2). We also investigated the effect of replacing one layer of the fiberglass batts with powder-filled evacuated panel (PEP) insulation. This advanced insulation had a nominal thermal resistance of 3.9 m²·K/W for a thickness of only 2.0 cm and eliminated the compressed insulation at the eave edge. It also greatly increased the level of the thermal resistance when used in the test attic. The idea was to better protect the edge thermally in order to prevent conditions for growth of mold, mildew or rot in the structure, especially near the outside corner of the building.

Figure 2 shows the location of seven thermocouples, labeled 'a' through 'g,' for information about local temperatures at the eave edge. Location 'a' was at the inside corner where the wall and ceiling met. Locations 'b' and 'd' were 3.8 cm from 'a.' Locations 'c' and 'e' were 7.6 cm from 'a.' Location 'f' was on top of the ceiling at the inside edge of the perimeter rail, halfway between trusses. Location 'g' was on the outside wall slightly below the top plate, halfway between studs. The inside and outside coefficients for convective heat transfer were adjusted in the model within limits suggested by heat transfer correlations until reasonable agreement was achieved between measured and modeled temperatures at 'a' through 'g.' When wall or deck sheathing was installed under the siding or roof, thermocouples, like ones at 'g,'

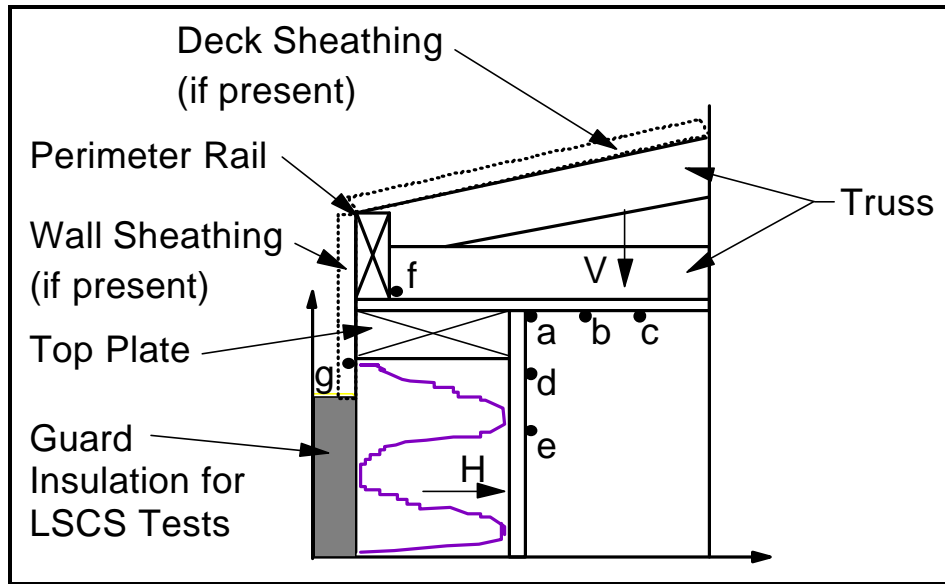


Figure 2. Detailed Schematic of the Eave Edge of the Manufactured Home Test Section

were again located on the outside after the siding or roof was replaced.

Figure 3 displays the temperatures at locations 'a,' 'c,' 'e,' 'f' and 'g' for four different insulation configurations. The specific data in Fig. 3 are for tests at a simulated winter condition of -17°C outside air temperature and 24°C inside air temperature with local surface temperatures presented in terms of the ratios $(T - T_{air\ out}) / (T_{air\ in} - T_{air\ out})$. Tests at outside air temperatures of -32°C and -3°C and the same 24°C inside air temperature showed the measured ratios to be the same as in Fig. 3 within ± 0.05 at worst. The model used thermal properties constant with temperature so the modeled ratios were independent of temperature.

Temperatures on the inside surfaces 'a,' 'c' and 'e' are not greatly different from the inside air temperature nor is the outside surface temperature 'g' greatly different from the outside air temperature. This is characteristic of wood-framed construction, even here where the gypsum

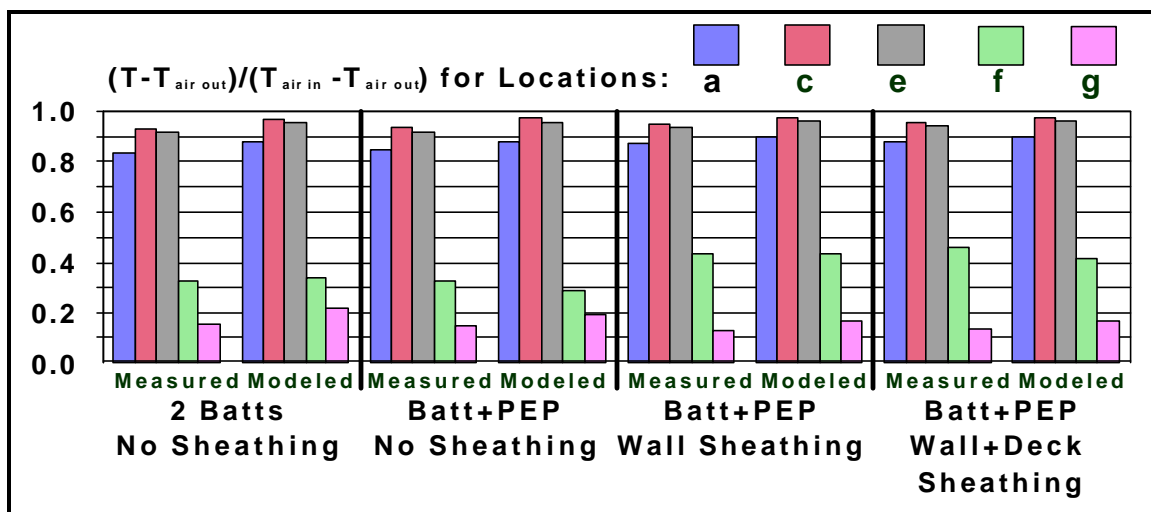


Figure 3. Measured and Modeled Local Temperatures at the Eave Edge of the Manufactured Home Test Section

ceiling causes a thermal bridge. The only temperature that changed significantly as more insulation was installed at the eave edge, but not until wall sheathing was installed, is that at location 'f' inside the attic at the edge of the perimeter rail. The use of the powder-filled evacuated panel insulation did not increase the temperature at 'f' nor increase the inside temperatures at 'a,' 'c' and 'e' above those with conventional insulation. Wall sheathing, consisting of 1.9-cm-thick extruded polystyrene installed under the aluminum siding to the top of the perimeter rail, made an improvement in the temperature at 'f' but not at 'a,' 'c' and 'e.' Deck sheathing, consisting of 1.9-cm-thick extruded polystyrene installed under the metal roof at the edge, did not improve any temperatures.

The significant feature shown by Fig. 3 is the consistent agreement between measured and modeled temperatures for all four configurations, with the modeled temperatures generally higher than the measured temperatures, but by about the same amount for all cases. Thus, the difference between inside and outside surface temperatures that drives the local heat transfer is the same for measurement and model. This is assumed to yield accurate estimates of the local heat transfer from the model. Direct measurement of three-dimensional heat transfer is difficult.

The model showed that 11% of the total heat flow rate for each configuration flowed horizontally through the stub of eave wall, comprising 2.5% of the test section area exposed to the metering chamber. It showed that 5% flowed vertically through the small part of the ceiling over which the conventional insulation was compressed between the ceiling and roof. This area comprised 1.4% of the test section area exposed to the metering chamber. The remaining 84% went through the rest of the ceiling, comprising 96.1% of the test section area exposed to the metering chamber. Consistent with the behavior of the temperature at 'f,' the total heat flow decreased as more and more insulation was added. The largest decrease was achieved by installing the wall sheathing. The practical conclusion for this building is that wall sheathing rather than powder-filled evacuated panel insulation improves its thermal performance most economically (Petrie et al. 1995).

Steel-framed Attic without and with Thermal Breaks

Another full-sized attic test section tested in the Large Scale Climate Simulator was a steel-framed half attic. The attic was constructed like a wood-framed attic with the ceiling gypsum board attached directly to the joists. The rafters, joists and wall top plate were joined directly at the eave edge with the rafters extending beyond to form an overhang for a soffit. A ventilation air system for the attic allowed air to flow into soffit vents and out a ridge vent. The vents were sealed for the test results shown in this example.

The upper photograph in Fig. 4 shows the details of the construction at the eave edge. Three levels of insulation were tested. The first, labeled R-3.3 in later figures, used full-width fiberglass batts with nominal thermal resistance of 3.3 m²·K/W and thickness of 15.9 cm between the 20.3 cm high joists. This left the top of the joists exposed in the attic. The second insulation level, labeled R-5.2, had a layer with nominal thermal resistance of 1.9 m²·K/W and thickness of 8.9 cm on top of the first layer. The thickness of the two layers exceeded the height of the joists but there was a small gap where the tops of the second layer of batts did not quite meet. The full width batts had to conform to the C-shaped framing. For the third insulation level, labeled R-7.1, another R-1.9 layer was added to the second. It was installed perpendicular to the joists and the joists were completely covered by the third layer.

The objective of tests with the steel-framed attic was to document the effect of the

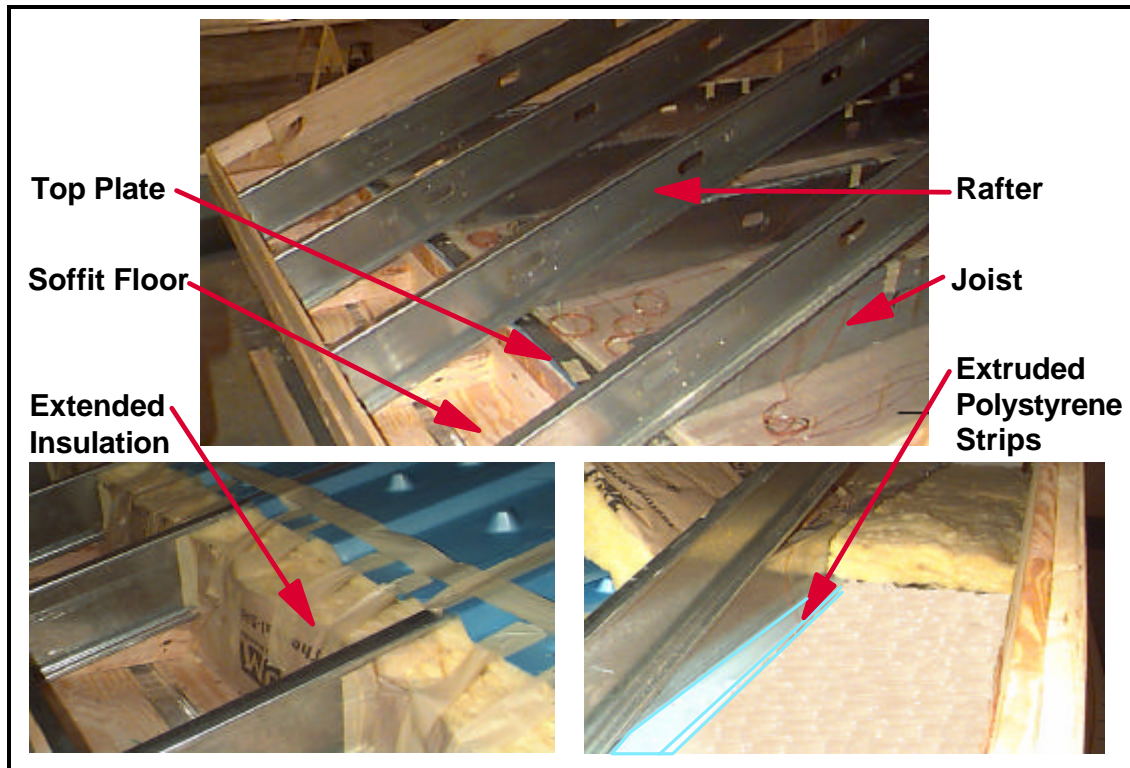


Figure 4. Photographs of the Steel-Framed Attic without Insulation (upper), with R-3.3 Fiberglass Extended over the Wall Top Plate (lower left) and with Fiberglass Batt Insulation (R-3.3 m²·K/W) Partially Installed between Joists plus 2.5 cm Thick Extruded Polystyrene Strips under the Joists (lower right)

thermal bridges through the joists and at the eave edge. Two modifications of the test section were undertaken to lessen the effect of these thermal bridges. For the first, as shown in the lower left photograph in Fig. 4, pieces of the R-3.3 fiberglass batt insulation were installed to extend the insulation over the top plate to the floor of the soffit. For the second modification, in addition to this added insulation, the ceiling was lowered and 2.5 cm thick by 10.2 cm wide extruded polystyrene strips were installed between the ceiling and the joists. The lower right photograph in Fig. 4 shows how the strips directly interrupt thermal bridges through the joists and ceiling.

Sets of thermocouples were located along the ceiling and in the attic at various places in order to measure the temperatures close to thermal bridges. One set was placed along the interior surface of the ceiling out from the inside edge of the eave wall halfway between the joists. Figure 5 presents temperatures at 1.9 cm, 4.4 cm, 7.0 cm and 12.1 cm from the eave wall and the average of several temperatures from thermocouples at least 30 cm from any thermal bridges (labeled 'far' in Fig. 5). All thermocouples were placed in the center of the test section halfway between the joists.

Data are shown for the three levels of insulation. For each level, there are the two modifications besides the basic, highly thermally bridged insulation. The temperatures shown were measured at winter conditions: -18°C outside air temperature and 21°C inside air temperature. With the attic vents sealed, attic air temperature is used as the reference instead of air temperature in the climate chamber.

From the trend displayed by the leftmost bar at each distance out from the wall, the

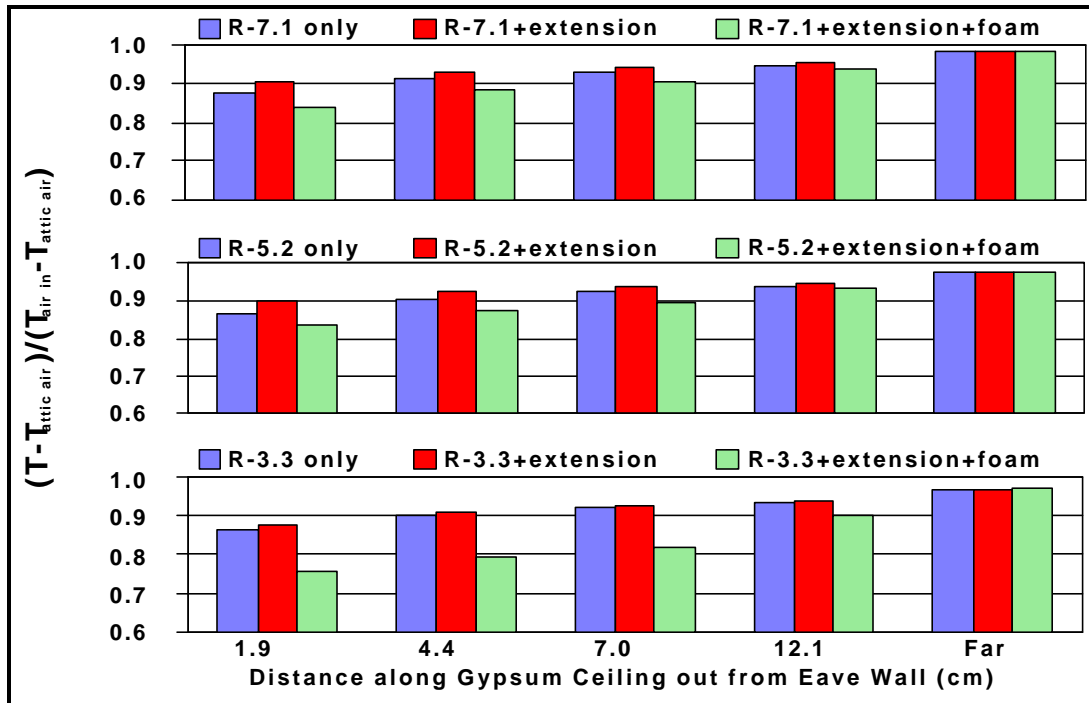


Figure 5. Thermal Bridge at Eave Wall of Steel-Framed Attic for Three Levels of Insulation (R-3.3, R-5.2 and R-7.1) plus Two Modifications for Each Level

severity of the thermal bridge is unaffected by the level of insulation. From the middle bars, extending insulation over the edge to the floor of the soffit does not help significantly. The total heat flow into the metering chamber bore out this observation, decreasing 1 to 2% for the tests with the extension compared to the base cases. Adding foam insulation under the joists lowered the ceiling by 2.5 cm. The rightmost bars show that this made the thermal bridge halfway between the joists at the eave wall more severe than it was in the unmodified cases. Foam should have been used, too, under the walls. The foam above the ceiling improved performance for the entire ceiling. The decrease in total heat flow for the R-3.3 case was 13% for the extension and foam compared to its base case (R-3.3 only). The decreases for the R-5.2 and R-7.1 extension and foam cases compared to their base cases were 11% and 7%, respectively.

Another set of thermocouples was placed on the ceiling at various distances from the center of a joist in the middle of the test section. From tests at winter conditions, Fig. 6 presents the temperatures at 0 cm, 1.3 cm, 2.5 cm, 5.1 cm, 7.6 cm and 12.7 cm from the center of a joist. The joists are 61 cm on centers. This thermal bridge in the middle of the attic is, as expected, unaffected by the extension of insulation over the eave edge to the floor of the soffit. Increasing the level of insulation in the attic itself is not an effective way to lessen the temperature depression on the ceiling under the joist. Insulating to the point of completely covering the joist, as the R-7.1 insulation does, is not as effective as adding the foam. The foam eliminates the thermal bridge regardless of attic insulation level, achieving dimensionless temperatures near 0.95 even under the joist

Foam-Core Concrete Parapet Wall

A final example of a test section for which local temperature measurements yield useful

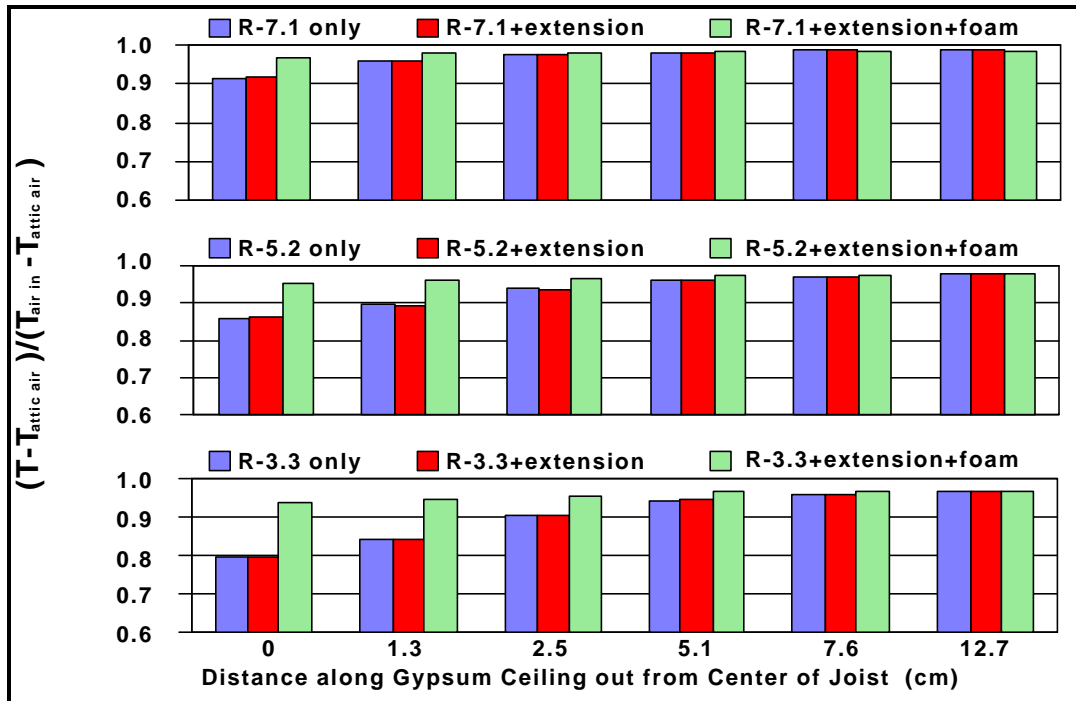


Figure 6. Thermal Bridge at Joists of the Steel-Framed Attic for Three Levels of Insulation (R-3.3, R-5.2 and R-7.2) plus Two Modifications for Each Level

information about thermal bridges is a mockup of a parapet wall that was tested in the Large Scale Climate Simulator. To achieve an acceptable R-value with concrete walls, it is common to include foam insulation elements. In the case of the parapet wall test section, a core of extruded polystyrene, 5.1 cm thick, is sandwiched between two 7.6 cm thick layers of high density concrete with appropriate reinforcing bars. The sandwich is held together by special thermally resistive ties so that the thermal resistance for heat flow in the horizontal direction of the wall itself is about 1.8 m²·K/W.

Of concern for these tests was how much extra heat flow the concrete would allow in the vertical direction when the concrete wall extended above the roof line to form a parapet. The ability of the Large Scale Climate Simulator to reproduce test conditions was relied upon for the test plan. First, a low-slope roof comprising a plywood deck and two layers of 2.5-cm-thick, high density fiberglass insulation was tested at severe winter conditions (outside air -18°C, inside air 21°C), mild winter conditions (outside air -1°C, inside air 21°C) and severe summer conditions (outside air 43°C, inside air 24°C). The roof R-value ranged from 2.3 to 2.2 m²·K/W. These tests were done with the roof on a special foam surround panel to extend the metering chamber walls vertically by 0.61 m. The metering chamber energy balance was corrected for heat flows through the metering chamber walls and this special foam surround panel to yield heat flow through the roof alone. The thermal conductivity of the foam comprising the surround panel was determined separately with a heat flow meter apparatus.

The vertical extensions allowed 0.61 m of the parapet wall to be inside the metering chamber. To accommodate the parapet wall a 20.3 cm wide slot was cut in two of the foam wall extensions. The wall extended 0.83 m above the roof, out of the center of which a 20.3 cm wide slot was also cut. Nailers were attached to the wall to support the divided roof. Figure 7 shows a photograph of the completed parapet wall test section with an inset to show the vertical

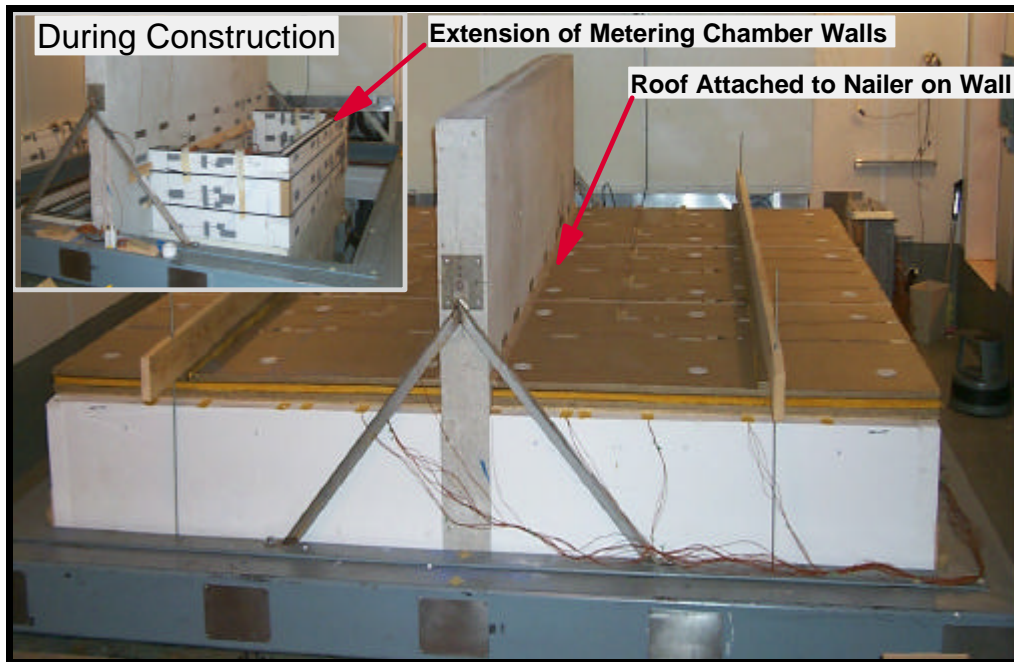


Figure 7. Photograph of Parapet Wall Test Section with Inset Photograph During Construction Showing Extension of Metering Chamber Walls and Nailer on Parapet Wall, Both to Support the Roof

extensions to the metering chamber and the nailer on one side. The wall rests on special supports, not shown underneath the assembly, to bear its considerable weight. The metering chamber was forced by jacks into good thermal contact with the bottom of the parapet wall.

The assembly in Fig. 7 was tested at the above severe winter, mild winter and severe summer conditions. The metering chamber energy balance was again corrected for heat flow rate through the metering chamber walls and the remainder of the surround panel. The heat flow rate through the remaining roof to the metering chamber at each condition was calculated by scaling the previous results for the roof without the parapet wall. Ratios of area times temperature difference with and without the parapet wall were used. Subtracting the scaled-down roof heat flow rate from the total heat flow through the remaining roof and the parapet wall yielded vertical heat flow rate through both of the concrete layers of the parapet wall.

The local temperatures measured on both sides of the parapet wall at various distances above and below the roof were symmetric within $\pm 1^\circ\text{C}$. Figure 8 shows these temperatures at various vertical positions on side 1 and side 2 of the parapet wall. Note that the values in the dimensionless form chosen for this paper are the same at each position regardless of severe winter, mild winter or severe summer conditions. These local temperatures, especially because of the relatively small difference between those at 4.4 cm above the roof and at 4.4 cm below the deck, are proof that a severe thermal bridge occurs. For the roof, with its thermal resistance of 2.2 to 2.3 $\text{m}^2\cdot\text{K}/\text{W}$, the dimensionless temperature was 0.04 on its top surface for these tests and was 0.94 on its bottom surface.

The symmetry of the temperatures convinced us that the vertical heat flows were equal on both sides of the mockup parapet wall. This allowed us to divide the vertical heat flow for the parapet wall by two and obtain an estimate of the effect for an actual parapet wall in which vertical heat flow only occurs for the inside layer of concrete. Below the roof line, where we imposed inside temperatures on both sides, an actual parapet wall would allow predominantly

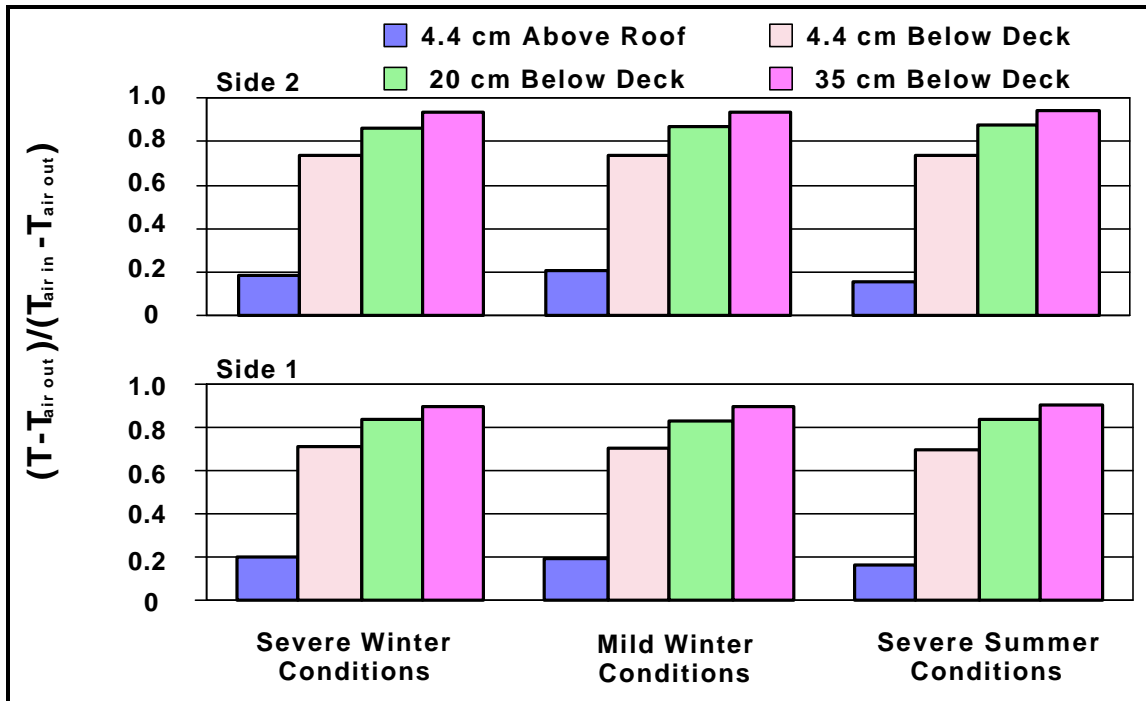


Figure 8. Surface Temperature Variations Vertically on Both Sides of a Foam-Core Parapet Wall for Severe Winter, Mild Winter and Severe Summer Conditions

horizontal heat flow. We have tested thermally efficient, foam-core concrete walls like this parapet wall. For foam-core concrete outside walls subject to the same air-to-air temperature differences as in the parapet wall tests, we estimated the heat flow per unit length through 2.4 m high walls. The extra heat flow through the parapet wall is 37% of the heat flow for the 2.4 m high wall at severe winter conditions (outside air -18°C , inside air 21°C). At severe summer conditions (outside air 43°C , inside air 24°C), the extra heat flow is 24% of the wall heat flow. The percentage varies linearly with temperature difference.

Conclusions

Local temperature measurements on full-size systems in laboratory hot box tests provide valuable insights into the location and severity of thermal bridges in complicated details that are part of the test systems.

- \$ Insofar as they validate three-dimensional models of details that exhibit thermal bridges, the local temperature measurements allow models to generate accurate estimates of local heat transfer through the details. Three-dimensional heat flow rate cannot be measured accurately by one-dimensional techniques, such as use of thin heat flux transducers.
- \$ When steps are taken to lessen the effect of the thermal bridges on thermal performance, local temperatures measured after improvements corroborate the expected improvements in performance measured by hot box techniques.
- \$ In a system for a hot box test, it is possible to replace complicated elements by simple elements that exhibit one-dimensional heat flow patterns. Measurement of temperature differences across simple elements with known thermal resistance and surface areas provides an accurate estimate of the heat transfer through the simple elements. The heat flow for the complicated elements can then be determined by analysis of the difference

between hot box test results for the system with the complicated elements and the system with the simple elements. The analysis requires that external air flows, air temperatures and all other features of the test section be identical for the two tests.

References

- ASTM. 1997. *Designation: C 1363-97. Standard Test Method for the Thermal Performance of Building Assemblies by Means of a Hot Box Apparatus*. West Conshohocken, Pa.: American Society for Testing and Materials.
- ASTM. 1989. *Designation: C 236-89. Standard Test Method for Steady-State Thermal Performance of Building Assemblies by Means of a Guarded Hot Box*. West Conshohocken, Pa.: American Society for Testing and Materials
- ASTM. 1990. *Designation: C 976-90 (Reapproved 1996). Standard Test Method for Thermal Performance of Building Assemblies by Means of a Calibrated Hot Box*. West Conshohocken, Pa.: American Society for Testing and Materials
- Christian, J.E., and J. Koňny. 1996. "Thermal Performance and Wall Ratings." *ASHRAE Journal*, 38 (3), 56-65.
- Koňny, J. and A.O. Desjarlais. 1994. "Influence of Architectural Details on the Overall Thermal Performance of Residential Wall Systems." *Journal of Thermal Insulation and Building Envelopes*, 18, 53-69.
- Petrie, T.W., J. Koňny, P.W. Childs, J.E. Christian and R.S. Graves. 1995. "Performance of Powder-filled Evacuated Insulation vs. Conventional Insulation in a Single-wide Manufactured Home Unit," 3-14. *Proceedings, Thermal Performance of the Exterior Envelopes of Buildings VI*. Atlanta, Ga.: American Society of Heating, Refrigerating and Air Conditioning Engineers.